MAGNETIC
RESONANCE
IMAGING

Neurophysiological and functional MRI evidence of reorganization of cortical motor areas in cerebral arteriovenous malformation

Francesca Caramia[a],*, Ada Francia[a], Caterina Mainero[b], Emanuele Tinelli[a],
Maria Giuseppina Palmieri[c], Claudio Colonnese[a], Luigi Bozzao[a], Maria Donatella Caramia[c]

[a]Department of Neurological Sciences, University of Rome "La Sapienza," 00185 Rome, Italy
[b]Athinoula A. Martinos Center for Biomedical Imaging, Massachusetts General Hospital, Harvard Medical School, Charlestown, MA 02129, USA
[c]Department of Public Health, University of Rome "Tor Vergata", Via Montpellier 1, 00133 Rome, Italy

Abstract

Functional magnetic resonance imaging (fMRI) research has shown that brain arteriovenous malformations (AVMs) lead to reorganization of cortical motor areas. Since it is known that blood oxygenation level-dependent signal in fMRI may be influenced by the hemodynamic perturbation associated with the presence of the AVM, in the present study, a combined exploration with fMRI and transcranial magnetic stimulation was performed in a patient with a right rolandic AVM in order to explore the relationship between neuronal and hemodynamic activity. The combined protocol of investigation adopted in this study was able to provide significant information regarding neuronal activity of the different cortical areas that partake to post-lesional reorganization.
© 2009 Elsevier Inc. All rights reserved.

Keywords: Cortical evoked potential; fMRI; Arteriovenous malformation

1. Introduction

Arteriovenous malformations (AVMs) are generally considered to be congenital vascular lesions even though there is an increasing evidence that the majority of cerebral AVMs develop postnatally and represent various types of endothelial cell dysfunction [1].

By means of functional magnetic resonance imaging (fMRI), it is possible to explore the functional reorganization which occurs in patients with AVMs. fMRI investigates brain function by mapping regional changes in blood oxygenation levels, in blood flow and/or volume in areas proximal to activated neurons. Therefore, any significant perturbation in brain hemodynamics would impact on fMRI results. AVMs dramatically alter normal cerebral circulatory dynamics even at sites remote from the AVM as well as in the contralateral hemisphere [2–9].

Transcranial magnetic stimulation (TMS) is able to explore directly the electrical activity of cortical neurons independently from cerebral hemodynamics, thus providing information exclusively on stimulated corticospinal projections.

We studied the effects of reorganization in a patient suffering from a right rolandic AVM, by using a combined exploration which included both TMS and fMRI, in order to achieve a comprehensive pattern of electrical and morphological changes.

2. Case report

A 33-year-old right-handed woman was admitted at our hospital for a sudden onset of paraesthesias of her left hand followed by loss of consciousness.

On admission, her neurological exam showed only mild clumsiness at left finger movements, but normal strength and sensitivity. She underwent a brain MRI that revealed the presence of an AVM extending from the right frontoparietal

---

to the temporal lobe. Cerebral angiography confirmed the diagnosis of arteriovenous malformation nourished by the middle cerebral artery.

She was then submitted to both fMRI and TMS to record motor evoked potentials (MEPs).

Five right-handed healthy age-matched volunteers, who underwent the same exploration procedures with fMRI and TMS, represented the control population.

All subjects were informed about the nature of the study and gave their written consent. This study was conducted in accordance with the ethical standards of the Committee on Clinical Investigation on Human Experimentation at our institution and with the Helsinki Declaration of 1964.

3. Methods

3.1. Functional MRI

fMRI data were acquired using a 1.5-T magnet (Gyroscan NT Intera; Philips Medical Systems, Best, The Netherlands) with echoplanar capabilities and a head volume radio-frequency coil. T2*-weighted echo planar images (64×64 matrix over a 24-cm field of view) consisting of 25 consecutive, 4-mm-thick axial sections, with TR/TE=3000/50 ms, a 90°flip angle and one excitation were then acquired.

During the fMRI acquisition, the subjects were asked to perform a self-paced sequential finger-to-thumb opposition task. Two fMRI trials (one for each hand) were obtained during the motor task.

After the fMRI study, proton density and T2-weighted spin-echo images (TR=2500 ms; TE=20/90 ms; two excitations) were acquired with the same geometry of the fMRI study (same slice orientation, contiguous 4-mm slices). fMRI data were analysed using SPM99 software (Wellcome Dept. of Cognitive Neurology, Institute of Neurology, London) according to the following procedure. In a preliminary analysis, patient's data were realigned and smoothed but not normalized and activation foci were superimposed on patients original T2-weighted images, so as to evaluate the exact spatial relationship between the AVM and the patients cortical areas. This preliminary procedure was aimed at investigating possible distortion caused by the malformation. After confirmation that no anatomical distortion was caused by the AVM for the final analysis images were realigned, normalized and spatially smoothed using a Gaussian kernel of 12 mm.

Statistical analyses were then performed using the principles of the general linear model extended to allow the analysis of fMRI data as a time series [10,11]. Statistical tests were then performed to determine signal changes that were significantly related to hand movement. Significance was determined on a voxel-by-voxel basis using a t statistic, which was then transformed into a normal distribution. Within each region of statistical significance, local maxima of signal increase were determined (the voxels of maximum significance), and their

location was expressed in coordinates (x, y and z) in the space of Tailarach and Tournoux [12]. Results were displayed using a statistical threshold of $P<.05$ corrected for multiple measures across the whole brain.

3.2. Transcranial magnetic stimulation

Stimulation of the cortex was performed by a Magstim 200 stimulator, connected to a figure-of-eight coil applied over the hand motor area (M1). The coil was held in a lateral orientation (45° from the midline) and moved on each hemiscalp over the central sulcus until the optimal site (hot spot) for eliciting motor responses in the *contralateral* hand target muscles, during relaxation, was localized at about 5 to 6 cm lateral to the vertex (indicated as Cz according to the 10–20 International system).

Ipsilateral MEPs were sought first by using the same spot as for *contralateral* MEPs (cMEPs) then moving the coil to a more medial region, with the center of the coil positioned at 3 cm lateral and 3 cm anterior to Cz, according to the methodology established in a study of Caramia et al. [13]. All MEP recordings were acquired by using 80% intensity of stimulator's output. This procedure was chosen in order to avoid excessive stimulation. Our purpose was then focused on picking up a large motor activation, including ipsilateral MEPs (iMEPs), attesting to the process of reorganization expected in the patient with respect to control subjects. Contralateral MEPs were simultaneously obtained. Therefore, measurements concerning cMEPs were also performed on recordings obtained (outside M1) from the stimulation of the "ipsilateral area" at 3 cm anterior and 3 cm lateral to Cz, with the same TMS intensity used for producing iMEPs [14].

3.3. MEP recordings

MEPs were recorded from thenar muscles (Opponens Pollicis) by using surface *disk electrodes taped* in a belly-tendon montage. The contraction of the target muscles consisted in a transient opposition of the thumbs, performed, bilaterally, at about 40% of maximal force (as measured via a force transducer). An acoustic feedback was also provided from the recording electrodes in order to monitor the electromyography (EMG) background. Recordings, averaged and replicated at least three times using a suitable amplitude calibration, were obtained with a Multibasis Esaote at a filter bandwidth and sampling rate of, respectively, 20–2000 Hz and 10 KHz and stored on floppy disks.

3.4. Transcranial magnetic stimulation data analysis

With TMS delivered at 3 cm lateral and 3 cm anterior to Cz, the following measurements were performed:

1. MEP latency onset measured at the beginning of the first reproducible negative deflection.
2. MEP amplitude measured from peak to peak.
3. MEP duration considered from the latency onset of the potential to its return to the baseline.

4. Silent period (SP) duration (ms) from the end of the MEP to the onset of EMG ongoing activity.

4. Results

Both fMRI and TMS yielded congruous results with respect to the position of local maxima of fMRI activation and hot spots for MEPs, involvement of ipsilateral activation and changes in both left (unaffected) and right (affected) hemispheres. These are principally characterized by: (1) presence of activation within the unaffected sensorimotor area ipsilateral to the moving hand and presence of iMEPs by stimulating the corresponding scalp sites; (2) functional displacement within the affected motor areas corresponding to polyphasic MEPs, attesting to reorganization and impulse scattering; (3) significant activation in secondary motor areas in both hemispheres.

fMRI has shown a significant alteration and enlargement of cortical motor areas, which was predominant in the unaffected hemisphere with a much greater ipsilateral activity than normal. TMS performed in positions corresponding to local maxima of fMRI analysis gave rise to a pattern of motor activation which matched the blood oxygenation level-dependent (BOLD) results, thus documenting that ipsilateral motor pathways extended from the unaffected left hemisphere to the left hand.

4.1. Functional MRI

Conventional T2-weighted MR images of the patient confirmed the presence of a large arteriovenous malformation located in the rolandic (precentral) region in the right hemisphere extending inferiorly to the right temporal lobe (Fig. 1). The conventional proton density and T2 weighted images also showed small foci of hyperintensity within the AVM, interpreted as perinidal gliosis; no signs of hemorrhage were observed.

4.1.1. Controls hand task

The fMRI study of control subjects revealed activation, which was predominantly located in the contralateral sensory-motor and pre-motor areas and in the ipsilateral cerebellum during either the movement of the right or of the left hand. Small foci of activation were also observed in the ispilateral motor areas, during the left hand movement in three of five subjects. A small cluster of activation was also observed in the ipsilateral premotor area during left hand movement in one control subject (#3) (Tables 1 and 2, Fig. 2 and Fig. 3).

4.1.2. Patient left hand task

In the patient, fMRI analysis demonstrated a large activation area which was mostly located in the ispilateral hemisphere during the left hand task, involving all motor areas (sensory-motor, pre-motor, supplementary motor, inferior parietal lobule and insula) and extended anteriorly and posteriorly with respect to the central sulcus (3 cm anteriorly and 2 cm posteriorly). The contralateral (right) hemisphere showed smaller and more scattered areas of significant activation, involving all motor areas and located above, superiorly, and posteriorly with respect to the AVM, both posteriorly and anteriorly with respect to the central sulcus (about 1 cm anteriorly and posteriorly). No BOLD signal could be detected within the nidus of the AVM (Fig. 1 and Fig. 2, Table 1).

4.1.3. Patient right hand task

In the patient, movement of the right hand determined a prevalent large contralateral activation, located in all motor

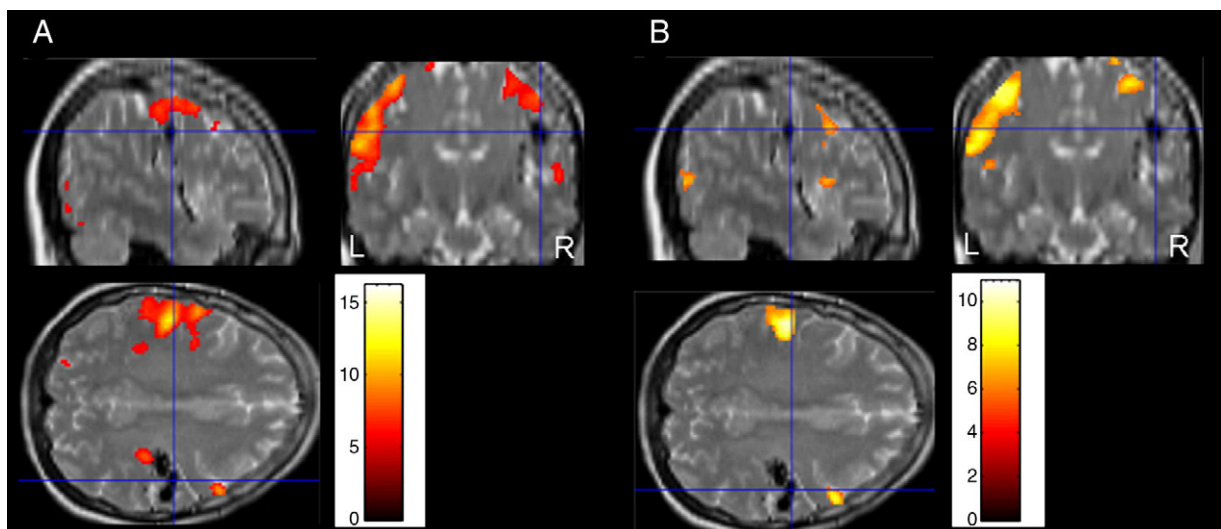Fig. 1. Activation areas obtained during either the left-hand (A) or the right-hand (B) movement superimposed on T2-weighted images in the patient harboring a right rolandic arterovenous malformation. Activation was predominantly in the left (unaffected) hemisphere during either hands movement. Smaller and more scattered foci of activation were observed around the AVM prevalently during the left hand movement.

Table 1
Locations of significant activation in controls and patient during left-hand movement

Region (BA)	Controls #1 Talairach coordinates (x, y, z)	Z	k	#2 Talairach coordinates (x, y, z)	Z	k	#3 Talairach coordinates (x, y, z)	Z	k	#4 Talairach coordinates (x, y, z)	Z	k	#5 Talairach coordinates (x, y, z)	Z	k	Patient Talairach coordinates (x, y, z)	Z	k
R sensory−motor (1−4)	48, −21, 45	6.05	100	50, −19, 53	5.41	34	51, −11, 52	6.88	256	32, −21, 49	5.95	57	57, −17, 41	5.77	11	38, −19, 47	7.36	685
	44, −12, 59	5.43	53										32,−21,50			59, 2, 9	6.01	20
	40,−36,53																	
R premotor (6)	30, −14, 69	7.06	137	22, −2, 60	6.05	25	40, −8, 64	6.69	352	32, −9, 49	5.98	82				36, −19, 49	7.08	576
				32, −16, 69	5.72	17										53, 15, 36	6.83	55
R parietal (40)	50, −40, 43	5.91	63										44, −50, 52	6.57	45	32, −53, 62	6.49	90
	40, −36, 53	5.50	14										45,−48,52			30, −33, 40	6.02	18
																34, −31, 37	5.78	12
																28, −36, 48	5.38	17
R insula							44, 2, −7	5.54	19				36, −11, 12	6.09	22	59, 4, 11	6.31	72
																38, −17, 12	6.01	38
																37, 10, 0	5.13	21
R cerebellum	22, −54, −26	5.17	35										40, −54, −24	5.92	19	26, −67, −20	7.64	946
SMA (6)																−8, 15, 66	6.80	77
L sensory−motor (1−4)	−44, −25, 40	5.27	12				−63,9,23	5.46	37				−65, −13, 15	6.29	13	−51, −19, 51	Inf	1671
							−40,−34,66	5.55								−36, −33, 70	5.69	18
L premotor (6)							−63, 9, 23	5.46	10							−59, 9, 27	Inf	1352
L parietal (40)	−56, −22, 29	5.48	16													−44 −32, 50	7.75	1184
L insula																−57, 23, −11	5.19	18
L cerebellum	−20, −50, −23	6.64	415	−26, −51, −18	6.71	227	−22, −57, −19	6.31	99	−22, −57, −14	6.54	434	−32, −63, −18	6.40	56	−16, −65, −15	Inf	855
	−20, −71, −17	5.46	35															
Vermis	14, −51, −14	5.31	12				0, −67, −13	6.99	16	−14, −47, −14	5.83	20	−4, −66, −3	7.17	34	−13, −65, −14	7.60	360
										−22, −59, −11	5.55	13						

BA, Brodmann area; R, right; L, left; SMA, supplementary motor area; Z, voxel-level corrected P value >.05; k, number of voxels, extent threshold K >10 voxels.

Table 2
Locations of significant activation in controls and patient during right-hand movement

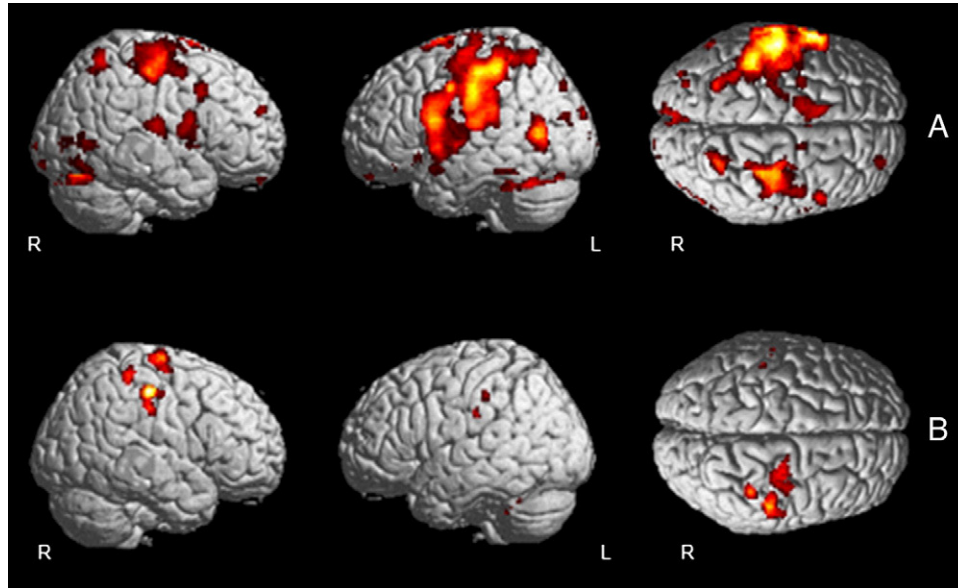| Region (BA)	Controls															Patient		
	#1			#2			#3			#4			#5					
	Talairach coordinates (x, y, z)	Z	k	Talairach coordinates (x, y, z)	Z	k	Talairach coordinates (x, y, z)	Z	k	Talairach coordinates (x, y, z)	Z	k	Talairach coordinates (x, y, z)	Z	k	Talairach coordinates (x, y, z)	Z	k
L sensory-motor (1–4)	−51, −13, 49	5.47	31	−46,−24,66	6.13	73	−44,−11,61	5.86	29	−40, −18, 58	6.44	11	−40, −14, 62	5.80	29	−55, −16, 34	7.22	1199
				−57, −19, 47	5.92	51												
L pre-motor (6)	−43, −13, 58	5.39	29				−42, −12, 63	5.79	125	−38, −12, 61	6.16	78				−36,−16,65	6.99	323
L parietal (40)	−56,−22,29	5.48	16													−44, −32, 50	7.75	1184
L cingulated (25–31)																−10, −65, 12	5.64	53
																−8, 15, −9	5.29	11
L insula																−63, 8, 10	6.53	333
																−57, −17, 16	6.00	63
L cerebellum	−22, −73, −18	5.42	27	−28, −50, −19	5.95	90				−20, −53, −19	6.64	271				−24, −63, −20	7.11	230
SMA (6)	−4, 14, 56	5.44	27													−6, 13, 62	6.23	130
	2, 16, 54	5.30	11													2, 9, 62	5.63	
																2, 11, 58	5.00	
R sensory-motor (1–4)																34, −21, 49	5.07	10
R premotor (6)																36, −16, 65	6.99	250
																16, −4, 72	6.92	38
																53, 13, 34	6.45	272
R insula																55, 6, 11	5.54	84
R cerebellum	14, −59, −16	7.01	522	12, −61, −15	5.73	49	20, −67, −17	6.46	270	22, −59, −15	6.65	314	38, −52, −24	5.64	13	24, −53, −19	6.23	484
										36, −83, −21	5.75	91						
Vermis	12, −61, −10	6.22	33				0,−67,−13	5.48	77	0, −63, −10	6.25	108				2, −65, −13	5.47	13
										−14, −71, −13	5.41	11						
										−6, −80, −11	5.09	12						

Fig. 2. Activation areas obtained during the left hand movement in the patient (A) and in a representative control subject (B) superimposed on a template volume rendering (both fMRI data and brain surface are normalized). Images show a predominant ipsilateral activation and a larger contralateral activation in the patient as compared to the control subject.

areas, including the cingulated gyrus. Smaller clusters of activation were seen in the ispilateral hemisphere, in the sensory-motor area, in a region anterior to the central sulcus (premotor area) and in the insula (Fig. 1 and Fig. 3, Table 2).

4.2. Transcranial Magnetic Stimulation

4.2.1. Controls

In 1 out of 5 control subjects only iMEPs could be elicited by stimulating the left hemisphere over pre-motor areas (3 cm lateral and 3 cm anterior to Cz), whilst no iMEPs could

be obtained during stimulation of M1. Such ipsilateral responses showed remarkably smaller amplitudes than those obtained in the patient and than cMEPs in all cases (Table 3).

No iMEPs were obtained during stimulation of the right hemisphere.

4.2.2. Patient

In the patient, large ipsilateral MEPs were recorded in response to stimulation of both hemispheres (Fig. 4 and Fig. 5). In contrast to normal subjects, the elicitation of such responses, was obtained not only by stimulating premotor
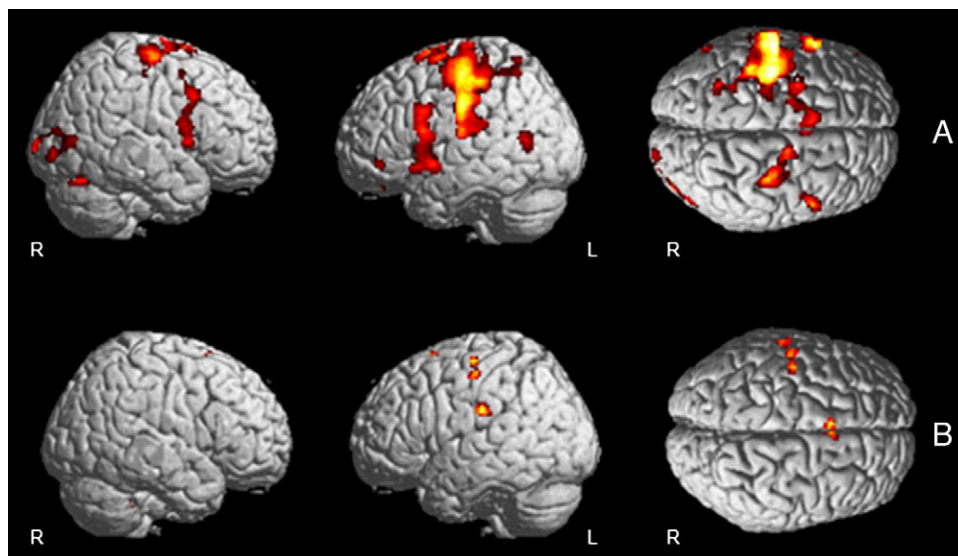

Fig. 3. Activation areas obtained during the right hand movement in the patient (A) and in a representative control subject (B) superimposed on a template volume rendering (both fMRI data and brain surface are normalized). Images show a larger contralateral activation in the patient as compared to the control and a small cluster of ipsilateral activation which is not evident in the control subject.

Table 3
TMS in control subjects and in the patient

M1	Controls				Patient			
	Left hemisphere		Right hemisphere		Left hemisphere (unaffected)		Right hemisphere (affected)	
Parameters measured	iMEPs	iMEPs	iMEPs	iMEPs	iMEPs	cMEPs	iMEPs	cMEPs
Amplitude (mV)	/	8.1±0.8	/	7.9±0.6	4.2±0.5	12.4±0.5	2.2±0.7	13.5±1.9
Latency (ms)	/	19.4±1.5	/	19.2±1.7	25.8±0.8	19.6±0.8	20.8±0.5	18±1.2
MEP duration (ms)	/	39.7±5	/	40.2±4.1	16.6±2.5	36.6±3.7	25±10	38.9±5.0
SP duration (ms)	/	135±10	/	139±8.7	20.7±9	142±19	16.6±8	147±25

Premotor								
Parameters measured	iMEPs	cMEPs	iMEPs	cMEPs	iMEPs	cMEPs	iMEPs	cMEPs
Amplitude (mV)	0.81±1.7	6.6±1.3	/	6.2±1.1	2.6±0.3	13.2±1.3	/	10±0.2
Latency (ms)	22.8±3	18.9±1.7	/	18.4±1.5	20.7±0.4	19.1±0.5	/	17.7±0.3
MEP duration (ms)	22.3±1	33.3±2	/	32.9±3	19.6±2.5	37.0±5.0	/	34.9±5.1
SP duration (ms)	21±11	145±10	/	146±9.2	29.1±11	140±15	18.3±5	138±18

/, recordings with MEPs not identifiable from background EMG activity. Measurements with means±S.D. are obtained during muscle contraction.

areas (position *b*), but also during stimulation of primary motor areas (position *a*) when exploring the unaffected left hemisphere, thus paralleling the emergent fMRI results. The stimulation of the right affected hemisphere gave rise to ipsilateral iMEPs from M1 whilst from the premotor site a poorly synchronized ipsilateral activity followed by a silent period could only be recorded (Fig. 4).

Large cMEPs, were obtained in both positions when stimulating both hemispheres. In particular, it is important to point up that amplitudes of cMEPs were all up to two times larger than normal and that cMEPs recorded in response to the affected right hemisphere showed a polyphasic morphology, i.e., loss of the normal triphasic morphology (Fig. 4); by stimulating the unaffected side cMEPs retained a normal morphology (Fig. 5; Table 3).

5. Discussion

In the present study, both fMRI and TMS testify a motor cortex reorganization in the context of a right rolandic arteriovenous malformation, consisting in a pattern of
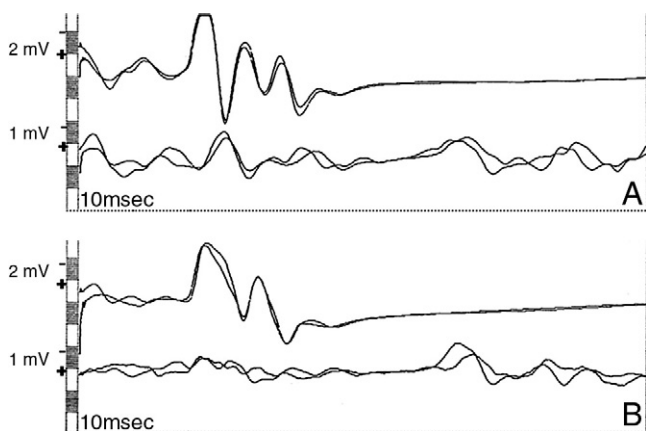

Fig. 4. TMS of the right (AVM) hemisphere. Traces displayed in the upper panel (A) relate to the stimulation of M1, where cMEPs (upper traces) morphology appear greatly poliphasic, reflecting the impulse scattering through the diseased/reorganized cortex; ipsilateral MEPs (lower traces) are also recorded, in contrast to normal, but with a lower amplitude than ipsilateral MEPs obtained from left (unaffected) hemisphere, as displayed in Fig. 5. Traces displayed in the lower panel (B) relate to stimulation of the premotor cortex, where cMEPs (upper traces) are still poliphasic, although less than in M1; ipsilateral MEPs (lower traces) are not so clearly identified from the background EMG activity.
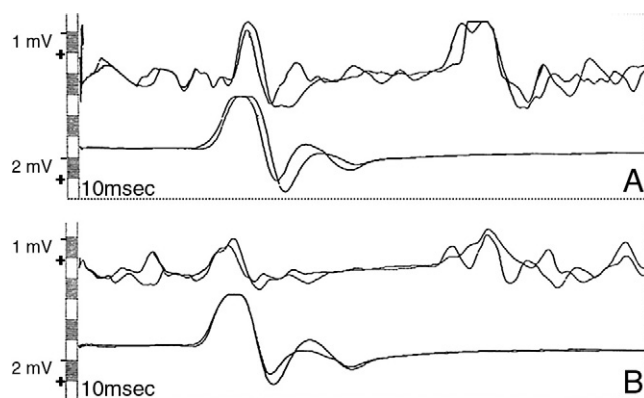

Fig. 5. TMS of the left (unaffected) hemisphere. Traces displayed in the upper panel (A) relate to the stimulation of M1, where iMEPs (upper traces) amplitude is the largest ever obtained amongst all iMEPs, recorded throughout all the stimulation sites on both hemispheres. This striking degree of ipsilaterality matches the predominant ipsilateral activation obtained during left hand movement in fMRI (Fig. 2). Contralateral MEPs (lower traces) were larger than normal, and even more so than iMEPs. Traces displayed in the lower panel (B) relate to stimulation of the premotor cortex, where iMEPs (upper traces) showed a lower amplitude than those recorded from M1; also in this position, cMEPs (lower traces) were both greater than normal and than ipsilateral ones.

predominant ipsilateral activity when moving the hand opposite to the affected hemisphere. The combination of the two techniques here allowed a wider view of motor information regarding our patient, who did not display motor deficits while harboring the AVM where motor areas are normally located and functionally activated.

The paradigm of crossed association, known as the Valsalva doctrine can be altered due to damage or disease, and the manifestation of ipsilateral activity reflecting a functional relationship between one hemisphere and the limbs on the same side of the body has been demonstrated in neurological patients during motor recovery [15–19].

Activation in ipsilateral motor cortex extended well beyond M1, including pre-motor, supplementary motor, parietal areas and insula. These results and the concurring generation of iMEPs both inside and outside M1 reflect an increased outflow of motor areas stimulation [20,21].

Ipsilateral activity expressed both by iMEPs and by fMRI activation foci could be also recorded in some control subjects, but on the left side only. This is in agreement with several studies and possibly reflects a physiological background of "ipsilaterality" with a bias towards left hemisphere bilateral motor control, showing that ipsilateral hemispheric activation is significantly greater with non-dominant (left) than dominant (right) hand motor tasks [22–24].

The presence of ipsilateral corticospinal connections appears to be a normal state in ontogeny, as demonstrated by a TMS study in healthy children. After cerebral damage, ipsilateral tracts may become unmasked by a lack of inhibitory control from the affected hemisphere or callosal output [25]. Contralateral activity was also recorded in our case, during movement of the left hand. Reorganization of contralateral cortical areas following injury to the adult brain has been described in several diseases, including stroke, multiple sclerosis, amyotrophyc lateral sclerosis and brain tumors. For lesions affecting the sensory-motor cortex, cortical changes classically involve enlargement of the limb cortical representation, anterior or posterior shift of the center of maximal activation, recruitment of other areas such as the insula and the parietal regions [16,26–31].

It has thus been proposed that the cortical generation and control of movements at the cortical level are mediated by parallel outputs from the nonprimary cortex as well as from the primary motor cortex [32]. As a consequence, several cortical neuron populations have the potential to influence the control of voluntary movements, independent of the proper M1.

Recovery of function after central nervous system damage depends on the maturity of the brain at the moment the damage is incurred, being generally greater when brain damage occurs early in life. These observations suggest that remaining areas of the brain are able to take over behavioral functions that normally occur in the damaged areas and that the brain possesses a greater ability to compensate in its immature than in its mature state. Our results are in accordance with findings of large-scale reorganization observed in primate studies. Rouiller et al. [33] demonstrated that both the stage of development at the time of an induced lesion and the extent of the lesion can play a major role in triggering different plastic changes contributing to the preservation of motor functions. In the immature brain, in which corticospinal projections have not yet reached their targets in the cervical cord, lesions in M1 mainly resulted in a functional shift to the ipsilateral, intact hemisphere. When lesions in M1 were induced in the mature brain, in contrast, a complete new map of hand and arm representation was found in a region adjacent to the lesion.

Although AVM are generally considered inborn errors of vascular morphogenesis, the exact period in which brain vascular malformations occur is still controversial. There is increasing evidence that they may develop postnatally, thereby representing a complex endothelial cell dysfunction [34]. The extensive contribution of the ispilateral, non-affected hemisphere to the execution of a motor task in our case suggests that the AVM may have been present early in the life of the patient. Furthermore, AVMs are often followed by later microhemorrhages or hemodynamic alterations that may have been responsible for later seizure-like activity.

Another aspect raised from our study is that no BOLD signal was present within the nidus of the AVM. As already observed by previous investigators, this condition could be explained by the histopathologic findings that the AVM's feeding vessels are separated from brain parenchyma and, therefore, do not participate to metabolic changes that occur during neuronal activity.

Alkhadi et al. [2] suggest that the conflicting results regarding the detection of BOLD signal within the nidus, as reported in some previous works, have to be related to the difficulty in distinguishing the exact border of the nidus so that the intervening brain interposed between the distal feeding and the proximal draining vessels could be mistaken for intranidal activation.

In our study, the aspects of cortical reorganization were concordantly demonstrated by both fMRI and TMS.

fMRI is a technique able to map functional activation by detecting changes in regional blood oxygenation levels, blood flow and volume. It is therefore extremely influenced by hemodynamic perturbations. A different characteristic of the BOLD response in the vascular network supporting the neuronal population of the damaged hemisphere may have contributed to the results. With respect to fMRI, TMS defines reorganization in terms of neural activity by inducing the activation of cortical regions, which manifests itself, directly, under the form of motor responses recorded in the target muscles. fMRI and TMS provide complementary information as to the status of the motor cortex. To optimize the meaning of the combined exploration, one has to consider, however, that activation visualized in fMRI parametric maps extended obviously beyond the foci explored with TMS. The hemodynamic response tends to

be more widespread in space and lasts longer in time as compared with the neuronal activity. This may be due to the characteristics of fMRI that preferentially provides information about intracortical processing or input to brain regions which are relevant for an actual task rather than the output of a region [35]. Therefore, when comparing the results of the two techniques, it should be taken into account the structural difference of the respective dominions of investigation: more spatial with fMRI that is like an open window; more temporal with TMS, where each event instantaneously related to the motor output is observed in a strictly focused dimension of space, like through a keyhole.

References

[1] Fleetwood IG, Steinberg GK. Arteriovenous malformations. Lancet 2002;359(9309):863–73.

[2] Alkadhi H, Kollias SS, Crelier GR, Golay X, Hepp-Reymond MC, Valavanis A. Plasticity of the human motor cortex in patients with arteriovenous malformations: a functional MR imaging study. AJNR Am J Neuroradiol 2000;21(8):1423–33.

[3] Latchaw RE, Hu X, Ugurbil K, Hall WA, Madison MT, Heros RC. Functional magnetic resonance imaging as a management tool for cerebral arteriovenous malformations. Neurosurgery 1995;37(4): 619–25 [discussion 625-616].

[4] Lehericy S, Biondi A, Sourour N, Vlaicu M, du Montcel ST, Cohen L, et al. Arteriovenous brain malformations: is functional MR imaging reliable for studying language reorganization in patients? Initial observations. Radiology 2002;223(3):672–82.

[5] Maldjian J, Atlas SW, Howard II RS, Greenstein E, Alsop D, Detre JA, et al. Functional magnetic resonance imaging of regional brain activity in patients with intracerebral arteriovenous malformations before surgical or endovascular therapy. J Neurosurg 1996;84(3): 477–83.

[6] Schlosser MJ, McCarthy G, Fulbright RK, Gore JC, Awad IA. Cerebral vascular malformations adjacent to sensorimotor and visual cortex. Functional magnetic resonance imaging studies before and after therapeutic intervention. Stroke 1997;28(6):1130–7.

[7] Thulborn KR, Davis D, Erb P, Strojwas M, Sweeney JA. Clinical fMRI: implementation and experience. Neuroimage 1996;4(3 Pt 3): S101–107.

[8] Valavanis A. The role of angiography in the evaluation of cerebral vascular malformations. Neuroimaging Clin N Am 1996;6(3): 679–704.

[9] Valavanis A, Yasargil MG. The endovascular treatment of brain arteriovenous malformations. Adv Tech Stand Neurosurg 1998;24: 131–214.

[10] Friston KJ, Frith CD, Frackowiak RS. Principal component analysis learning algorithms: a neurobiological analysis. Proc Biol Sci 1993; 254(1339):47–54.

[11] Friston KJ, Holmes AP, Poline JB, Grasby PJ, Williams SC, Frackowiak RS, et al. Analysis of fMRI time-series revisited. Neuroimage 1995;2(1):45–53.

[12] Talairach J, Tournoux P. Co-planar stereotaxic atlas of the human brain: 3 dimensional proportional system; an approach to cerebral imaging. Stuttgart: George Thieme Verlag; 1988.

[13] Caramia MD, Telera S, Palmieri MG, Wilson-Jones M, Scalise A, Iani C, et al. Ipsilateral motor activation in patients with cerebral gliomas. Neurology 1998;51(1):196–202.

[14] Caramia MD, Palmieri MG, Giacomini P, Iani C, Dally L, Silvestrini M. Ipsilateral activation of the unaffected motor cortex in patients with hemiparetic stroke. Clin Neurophysiol 2000;111(11):1990–6.

[15] Lee M, Reddy H, Johansen-Berg H, Pendlebury S, Jenkinson M, Smith S, et al. The motor cortex shows adaptive functional changes to brain injury from multiple sclerosis. Ann Neurol 2000;47(5):606–13.

[16] Nyberg G, Andersson J, Antoni G, Lilja A, Pellettieri L, Valind S, et al. Activation PET scanning in pretreatment evaluation of patients with cerebral tumours or vascular lesions in or close to the sensorimotor cortex. Acta Neurochir (Wien) 1996;138(6): 684–94.

[17] Reddy H, Narayanan S, Arnoutelis R, Jenkinson M, Antel J, Matthews PM, et al. Evidence for adaptive functional changes in the cerebral cortex with axonal injury from multiple sclerosis. Brain 2000;123 (Pt 11):2314–20.

[18] Rocca MA, Falini A, Colombo B, Scotti G, Comi G, Filippi M. Adaptive functional changes in the cerebral cortex of patients with nondisabling multiple sclerosis correlate with the extent of brain structural damage. Ann Neurol 2002;51(3):330–9.

[19] Vinas FC, Zamorano L, Mueller RA, Jiang Z, Chugani H, Fuerst D, et al. Diaz FG. [15O]-water PET and intraoperative brain mapping: a comparison in the localization of eloquent cortex. Neurol Res 1997;19 (6):601–8.

[20] Leblanc E, Meyer E, Zatorre R, Tampieri D, Evans A. Functional PET scanning in the preoperative assessment of cerebral arteriovenous malformations. Stereotact Funct Neurosurg 1995;65(1-4): 60–4.

[21] Morioka T, Yamamoto T, Mizushima A, Tombimatsu S, Shigeto H, Hasuo K, et al. Comparison of magnetoencephalography, functional MRI, and motor evoked potentials in the localization of the sensory-motor cortex. Neurol Res 1995;17(5):361–7.

[22] Bastings EP, Gage HD, Greenberg JP, Hammond G, Hernandez L, Santago P, et al. Co-registration of cortical magnetic stimulation and functional magnetic resonance imaging. Neuroreport 1998;9(9): 1941–6.

[23] Johansen-Berg H, Rushworth MF, Bogdanovic MD, Kischka U, Wimalaratna S, Matthews PM. The role of ipsilateral premotor cortex in hand movement after stroke. Proc Natl Acad Sci U S A 2002;99(22): 14518–23.

[24] Lotze M, Kaethner RJ, Erb M, Cohen LG, Grodd W, Topka H. Comparison of representational maps using functional magnetic resonance imaging and transcranial magnetic stimulation. Clin Neurophysiol 2003;114(2):306–12.

[25] Caramia MD, Iani C, Bernardi G. Cerebral plasticity after stroke as revealed by ipsilateral responses to magnetic stimulation. Neuroreport 1996;7(11):1756–60.

[26] Baumann SB, Noll DC, Kondziolka DS, Schneider W, Nichols TE, Mintun MA, et al. Comparison of functional magnetic resonance imaging with positron emission tomography and magnetoencephalography to identify the motor cortex in a patient with an arteriovenous malformation. J Image Guid Surg 1995;1(4):191–7.

[27] Carpentier AC, Constable RT, Schlosser MJ, de Lotbiniere A, Piepmeier JM, Spencer DD, et al. Patterns of functional magnetic resonance imaging activation in association with structural lesions in the rolandic region: a classification system. J Neurosurg 2001;94(6): 946–54.

[28] Morioka T, Mizushima A, Yamamoto T, Tobimatsu S, Matsumoto S, Hasuo K, et al. Functional mapping of the sensorimotor cortex: combined use of magnetoencephalography, functional MRI, and motor evoked potentials. Neuroradiology 1995;37(7):526–30.

[29] Mueller WM, Yetkin FZ, Hammeke TA, Morris III GL, Swanson SJ, Reichert K, et al. Functional magnetic resonance imaging mapping of the motor cortex in patients with cerebral tumors. Neurosurgery 1996; 39(3):515–20 [discussion 520-511].

[30] Nishiyama Y, Yamamoto Y, Fukunaga K, Satoh K, Ohkawa M, Kunishio K, et al. Visualization of the motor activation area using SPECT in neurosurgical patients with lesions near the central sulcus. J Nucl Med 2000;41(3):411–5.

[31] Schreiber A, Hubbe U, Ziyeh S, Hennig J. The influence of gliomas and nonglial space-occupying lesions on blood-oxygen-level-

dependent contrast enhancement. AJNR Am J Neuroradiol 2000;21(6): 1055–63.

[32] Dum RP, Strick PL. The origin of corticospinal projections from the premotor areas in the frontal lobe. J Neurosci 1991;11(3):667–89.

[33] Rouiller EM, Yu XH, Moret V, Tempini A, Wiesendanger M, Liang F. Dexterity in adult monkeys following early lesion of the motor cortical hand area: the role of cortex adjacent to the lesion. Eur J Neurosci 1998;10(2):729–40.

[34] Stapleton SR, Kiriakopoulos E, Mikulis D, Drake JM, Hoffman HJ, Humphreys R, et al. Combined utility of functional MRI, cortical mapping, and frameless stereotaxy in the resection of lesions in eloquent areas of brain in children. Pediatr Neurosurg 1997;26(2): 68–82.

[35] Logothetis NK, Pauls J, Augath M, Trinath T, Oeltermann A. Neurophysiological investigation of the basis of the f MRI signal. Nature 2001;412(6843):150–7.